Automation in Construction 173 (2025) 106107

Contents lists available at ScienceDirect

Automation in Construction

journal homepage: www.elsevier.com/locate/autcon

Optimized crane mat design and transit path planning using a graph search algorithm

Monjurul Hasan [a], Ming Lu [b,*]

[a] Transportation and Economic Corridors, Government of Alberta, Twin Atria Building, 4999 98 Ave NW, Edmonton, Alberta T6B 2X3, Canada

[b] Department of Building and Real Estate (BRE), Faculty of Construction and Environment (FCE), The Hong Kong Polytechnic University, Hung Hom, Kowloon, Hong Kong

A R T I C L E I N F O

Keywords:
Temporary design in construction
Optimization
Crawler crane
Mat design
Mat layout planning
Crane path planning

A B S T R A C T

Designing temporary crane transit paths in large construction sites with varying geological profiles presents two challenges: (1) ensuring safe, efficient, and cost-effective operations, and (2) developing optimization solutions that consider material properties, ground loading, and site layout. This paper addresses these challenges by integrating a graph search algorithm with crane mat structural design to optimize crane mat layouts and transit paths. A case study of structural steel subassembly installations, based on a real-world project, demonstrates the method's effectiveness. The results highlight safety-focused crane mat designs and transit plans, along with significant cost savings compared to traditional heuristics.

1. Introduction

Modular construction entails dividing a large structure into manageable components to be prefabricated in a controlled environment and subsequently shipped for installation in the construction field. While this method alleviates the productivity-inhibiting factors inherent in on-site "stick-build" construction, the subsequent assembly of these modules requires strict adherence to engineered procedures to maintain the integrity of the final structure while ensuring worker safety [1]. As modular construction technology advances, there is an increasing trend in maximizing module functionality, leading to heavier modules weighing tens to hundreds of tons [2]. Consequently, the combined pressure exerted by the crane and its payload on the ground also substantially increases. This trend necessitates the development of advanced lifting equipment, including cranes, mats, and rigging gears, capable of handling these increased loads [3].

To ensure safe operations of cranes, it is vital to verify that the ground's bearing capacity can accommodate the combined weight of the crane and its payload. This process involves geotechnical characterization of the existing ground conditions and enhancing ground-bearing capacity using engineered devices, such as ground mats or soil stabilization techniques [4]. One common method to improve ground bearing capacity is the use of mats (e.g., timber blocks, steel plates), with their size and thickness determined through engineering principles based on analysis of the load and existing soil bearing capacity [5]. While designing ground mats is essential, a proper mat layout plan minimizes crane movements and enhances operational efficiency and safety [6,7]. The mat layout plan explicitly specifies the size and thickness of the mats as well as the locations of placement in the field. In addition, implementing a mat layout plan requires the use of special equipment, such as trailers and forklifts, to transport and set up the mats from the storage yard to the construction site. After completing crane operations, these mats are removed and returned to the mat yard for reuse on the next lift. In short, the mat installation and removal operation would have serious safety implications and incur considerable field overhead costs, thus warranting meticulous planning.

Practitioners in the field typically utilize computer-aided design and drafting (CADD) software to prepare crane mat layout plans, relying on an intuitive approach to minimize crane travel distances [8]. The primary objective is to minimize the volume of mats used in order to cover the maximum required area in local installation sites where crane movement is subject to site constraints [9,10]. These layout plans are designed to consider site conditions and avoid obstacles that could interfere with the lifted module or the crane. However, on major industrial or infrastructure construction projects, fabricated modules are custom-made and of considerable size. These modules are rarely transported directly to the site due to transportation and logistics constraints. Instead, they are delivered as smaller, manageable modules that require

* Corresponding author.
E-mail addresses: monjurul.hasan@gov.ab.ca (M. Hasan), m-ing.lu@polyu.edu.hk (M. Lu).

https://doi.org/10.1016/j.autcon.2025.106107
Received 31 July 2024; Received in revised form 26 February 2025; Accepted 27 February 2025
Available online 6 March 2025

further assembly on-site in a yard before installation [11]. When these smaller modules are pieced together into subassemblies, they become so heavy that a meticulous plan is required to transit a subassembly from the on-site fabrication yard to the installation location. This planning process generally entails a site geological survey to assess the ground-bearing capacity and design crane mat layout along the transit path. The mat, as laid out, adds to the existing ground-bearing capacity to withstand the crane's gross weight and payload in operation. Additionally, site constraints such as crane movement restricted areas and ground surface contour also impede operational efficiency and impact crane stability, which need to be considered in crane transit path planning. While comprehending the shortest path from an assembly yard to an installation location without accounting for the ground bearing capacity can be straightforward, the decision process becomes inadequate given the crane load is high, the ground soil profile is complex and multiple path alternatives are practically feasible. Under such circumstances, selecting the shortest path may not always yield the most economical outcome. The existing literature lacks a comprehensive analytical approach for crane transit path planning over relatively long distances that aims to achieve the maximum cost efficiency while ensuring safety and minimizing costs.

This paper introduces an automated approach for preparing crane mat layout plans, considering ground engineering properties (i.e. ground bearing capacity), crane operation safety (i.e. crane speed), and mechanical properties of materials selected for ground mat design. In contrast with commonly practiced empirical methods, the proposed algorithm automates this entire process, reducing preparation time to a few seconds. Relying on graph theory, the algorithm generates an optimum mat layout plan that specifies the width and thickness of mats used and lays out the crane transit path. This automated approach optimizes crane mat usage and crane transit path coverage while ensuring safety and cost efficiency (in terms of mat use and crane operation costs), eliminating the need for practitioners to manually adjust crane mat layout plans. With this approach, practitioners would potentially achieve the optimum solution on the first attempt, thereby enhancing efficiency and reducing rework.

The remainder of this paper first presents a critical review of the literature on the identified research problem. Next, the analytical method for mat design for mobile cranes (crawler cranes) is introduced, which combines the graph search algorithm, specifically Dijkstra's algorithm, to tackle the problem of crane mat layout planning. The design equations are devised explicitly for crawler crane mats made of steel or aluminum-which can be readily adapted for timber blocks with minor modifications [12]. To account for practical needs, the proposed method considers site constraints for crane movement, mat material costs, and crane operation costs (setup and movement) in order to achieve the highest construction cost efficiency. It is pointed out that the ground profiles for a construction site, including both the geotechnical profile (soil bearing capacity) and the surface profile (path slope), feeds into the optimization in order to ensure the stability of the crane. A case study demonstrating the step-by-step application of the proposed methodology is presented, conclusions of this research are drawn, and further extensions discussed at the end.

2. Problem background and critical review

2.1. Crane stability against ground pressure

With ground stability being a critical concern, safe operations of heavy cranes on a construction site demands the proper use of ground support. According to the United States Occupational Safety and Health Administration, between 2000 and 2009, approximately 8.76 % (50 of 571 total) of fatal accidents in the United States were attributed to cranes tipping over, a direct result of inadequate ground support [13]. Between 2004 and 2010, the number stayed at around 28 % (21 of 75 total) [14]. Statistics indicate that ground stability is one of the most crucial issues in crane operations. Among all types of cranes, mobile cranes are identified to be more prone to tipping over. During 1997–2003 in the US, 84 % of all the fatalities involving cranes/derricks were attributed to mobile cranes [15]. Data from the U.S. Bureau of Labor Statistics (2011–2017) shows that 43 % of fatal crane-related work injuries occurred in the private construction industry, primarily among specialty trade contractors and heavy and civil engineering sectors. Crane operators accounted for 15 % of these fatalities [16]. Similarly, crane operation safety is a growing concern in Canada, with British Columbia alone reporting 22 crane-related incidents in the past three years [17]. An investigation of crane accidents between 2011 and 2015 found that mobile crane overturning represented 45 % of all crane accidents [18]. Other related studies also identified stability failure as the major source of crane accidents [19,20,21].

Despite numerous crane accidents, crawler cranes remain a favored choice on major construction projects due to their capacity to lift substantial structures and travel with payloads [6]. Given the critical role that crawler cranes play in construction, it is imperative for construction planners to ensure that the soil-bearing capacity of the ground be adequate to support the combined weight of the crane and its payload. At present, common methods are applicable to address inadequate soil-bearing capacities include (1) using compacted aggregates as a means of ground improvement to increase its bearing capacity; (2) using crane mats designed by engineering principles to distribute the crane's ground-bearing pressure more evenly, thereby reducing the required soil-bearing capacity. Typically, for high-capacity cranes, lift engineers combine both techniques (i.e., soil stabilization using compaction and crane mats) for the sake of safety of lifting operations. It is noteworthy that laying mats provides a more economical choice as they are reusable, unlike ground improvement for crane transit [22,23]. Hence, this research focuses on preparing mat designs against the existing ground bearing capacity, which is determined through performing geotechnical sampling and testing (such as standard penetration test).

2.2. Crane mat layout planning

Planning construction operations involving mobile cranes presents a multifaceted problem in construction engineering relevant to time, cost, safety, and productivity [24]. The literature heavily emphasizes crane lift planning, which is a complex combinatorial optimization problem addressing crane selection, identifying optimal locations on congested sites, and avoiding potential collisions [25,26]. However, research on crane transit path planning for heavy lifts over considerable distances is still lacking. Reddy and Varghese [27] developed a tool using configuration space (C-space) to identify and optimize crane lift paths within a constrained search space. Ali et al. [28] proposed a genetic algorithm-based approach for automated path planning of mobile cranes. Lin et al. [29] improved the bidirectional Rapidly Exploring Random Trees (RRTs) algorithm to speed up the processing for optimal path design. Peng et al. [30] explored the interaction between construction site crews and mobile cranes to produce optimal crane transit plans.

While crane operation optimization has received increasing attention in recent years, the optimization of crane transit path planning, considering the site's geometric profile (contour) and geotechnical properties of the ground, remains under-researched. Planners usually specify crane mat requirements based on the mobile crane's ground-bearing pressure and the soil-bearing capacity on the construction site; but often overlook the optimization of crane mat utilization in bulk [31]. Taghaddos et al. [7] proposed a comprehensive crane optimization framework encompassing crane positioning, rigging gear optimization, lift optimization, crane path optimization, and crane mat requirements, but it fell short to address crane mat optimization specifically. This research gap is significant, considering that crane mats play a critical part in safe and productive operations on many construction sites while also exerting substantial influences on project time and cost performances. Simulation modeling was applied to analyze the complexity of lift operation planning in a dynamic environment to ensure operational safety. However, the critical aspect of required crane mat design and layout planning, essential to confirm stability and ensure overall operational safety, had largely been overlooked [8,32]. Furthermore, Aghajamali et al. [33] proposed an algorithm for the optimized planning of crane walking-involved lift operations, incorporating an obstacle avoidance technique adapted from robotics. Yet, the research was primarily focused on ensuring the safety of the lifting process, without addressing the broader issues of crane mat planning optimization or stability-related safety. Another notable attempt by Ali et al. [6] coupled an agent-based greedy algorithm with reinforcement learning to obtain global optimization of crane mat plans on site; the objective function reduced crane mat material use and crane movement simultaneously. It is noteworthy that most planning algorithms proposed in reviewed research are intended for stationary or short-haul problems (crane movement confined to areas adjacent to the installation site), falling short in considering (1) ground surface profiles (i.e., contours and slopes) that affect crane stability and speed and (2) geological profiles of the site area (i.e. soil bearing capacity) in determining mat size and thickness.

In the field of site layout optimization, researchers developed methods to aid practitioners in determining optimal crane locations, considering safety, time, and cost constraints. Optimization algorithms and configuration space analysis were proposed for automated path planning of mobile cranes, aimed to identify space-occupying conflicts within site boundaries [34,10,35]. Site mat design optimization for crane movement was also addressed in the literature [6,31]. In large site areas where cranes operate on the ground made of varying geological profiles, designing temporary crane transit paths presents both (1) a distinctive challenge to plan safe, efficient, and cost-effective construction operations and (2) a unique research opportunity to formulate optimization solutions factoring in material mechanical properties, ground loading analysis, site layout planning. To address this gap in knowledge and practice, the present study proposes an approach for optimizing crane mat layout by integrating a graph search algorithm with the structural design of crane mats in efforts to facilitate the preparation of crane mat design and transit path planning in a construction field.

2.3. Graph search algorithm

Graph search algorithms provide fundamental quantitative techniques extensively used for solving problems related to network analysis, pathfinding, and optimization in operations research and artificial intelligence. Various graph search algorithms were developed, each featuring unique advantages and special applications [36]. Graph search algorithms evolved significantly over time. Each variant was adept at addressing specific challenges. Depth-First Search (DFS) and Breadth-First Search (BFS) provided fundamental traversal techniques with distinct advantages in memory usage and pathfinding, respectively [37]. The *Dijkstra's Algorithm*, developed by Edsger W. Dijkstra in 1956, is a cornerstone in the operations research field for addressing the shortest path optimization problems. It uses a priority queue to explore the shortest path from a source vertex to all other vertices in a weighted graph [38]. The major advantage of Dijkstra's Algorithm lies in its ability to handle graphs with nonnegative weights efficiently, making it indispensable for applications in routing and navigation systems [39]. In short, Dijkstra's Algorithm offers an efficient solution for shortest path problems represented in weighted graphs, while the *A* Search Algorithm* enhances pathfinding efficiency with heuristic guidance. Understanding the development and advantages of these algorithms is a prerequisite to leveraging their respective strengths in various applications across computer science and artificial intelligence.

Applications of graph search algorithms in civil engineering domains are as follows: graph search algorithm was used in solving the shortest path problem for large-scale transportation network [40]; Sivakumar et al. [41] used A* Search Algorithm for automating the process of crane path planning where two cranes interacted with each other; Performances of water distribution systems were evaluated by graph search theory [42]; Liu and Lu [43] proved the concept of using Dijkstra's Algorithm for temporary haul road layout design for massive rough grading projects; El Meouche et al. [44] used the Dijkstra's Algorithm to find the optimal paths for evacuating risky construction sites. It is noteworthy that the classical algorithm originated from operations research and mathematical optimization, which had been more commonly applied in the specialty of transportation in civil engineering. In construction engineering and project management, Dijkstra's graph search was less explored [35]. In this paper, the algorithm application is streamlined and embedded in the problem definition of crane mat design and transit path planning, factoring in material mechanical properties, ground loading analysis, site layout planning, geotechnical investigation, method planning and cost estimating. In particular, this present study resorts to the Dijkstra's Algorithm to solve the optimization problem of crane mat layout planning considering mat engineering design and the site ground profiles, namely: the geotechnical profile (soil bearing capacity) and surface profile (ground slope).

3. Proposed approach

3.1. Formulation of crane mat design

The design of crane mats is a multifaceted process requiring a thorough understanding of fundamental knowledge of structural and geotechnical engineering. Crane mats are designed to distribute the crane load uniformly to the ground as shown Fig. 1. The crane mat size A_{req} needs to be adequate so that the load distributed by the mat q does not exceed the ground allowable bearing pressure $q_{a,}$ as given in Eq. (1). For this study, q_a is considered between 30 % to 50 % (factor of safety FS = 2 to 3) of the ground bearing capacity q_g (Eq. (2)).

$$A_{req} = \frac{P + P_W}{q}; where\ q \leq q_a \tag{1}$$

$$q_a = \frac{q_g}{FS} \tag{2}$$

In Eq. (1), P is the total crane load applied to one mat, P_W is the mat weight. Initially, the total ground stress q due to the lift total $(P + P_W)$ is assumed to be equal to the allowable ground pressure $q_{a,}$ derived from soil geotechnical investigation using Eq. (2). At the beginning of the design, the weight of the mat itself is difficult to guess without knowing the mat material thickness t. Therefore, the approach is to estimate the effective length of the mat material L'_{eff} first, then proceed through the iterative process to select a mat with a specific thickness that is sufficient for the ultimate ground bearing capacity q_g. This iteration starts with finding the bearing pressure, ignoring the weight of the mat using Eq. (3), where the crane track width is B. At the end of the trial, the effective mat length L_{eff}, which is greater than the effective mat length L'_{eff} found in the final trial, needs to be considered for design. Therefore, the actual bearing pressure under the mat can be fixed using Eq. (4). It is important to note that if a mat with width b is used to support the crane's track, and n mats are required to support the crane, the load will be distributed across all the mats supporting the crane. Therefore, in the design, the total effective width B will be considered as $(n \times b)$ instead of the crane track width.

$$L'_{eff} = \frac{P}{q_a B} \tag{3}$$

$$q = \frac{P}{L_{eff} B} \tag{4}$$

If C is the width of the crane chain track, Eq. (5) provides the length of the cantilever portion of the mat L_c. The maximum moment M for this

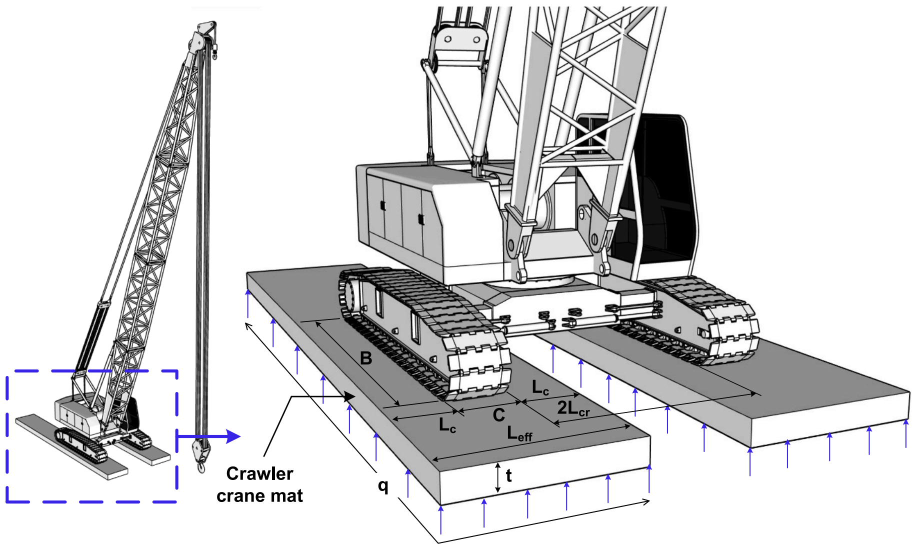

Fig. 1. Load distribution under the crawler crane track.

cantilever portion can be found using Eq. (6),

$$L_c = \frac{L_{eff} - C}{2} \tag{5}$$

$$M = \frac{1}{2}(L_c)^2(qB) \tag{6}$$

Now, with maximum moment M under the crane mat and the allowable bending stress F_{ab} (Eq. (7)) for the mat material known (60 % of the yield strength F_y for steel and aluminum), the thickness of the mat can be found from Eq. (8).

$$F_{ab} = \frac{Mc}{I} = \frac{M}{S} = \frac{M\frac{t}{2}}{\frac{Bt^3}{12}} = \frac{6M}{Bt^2} \tag{7}$$

$$t = \sqrt{\frac{6M}{BF_{ab}}} \tag{8}$$

Here, I is the moment of inertia of the mat section, c is the distance from the centroid to the extreme fiber of the beam, and S is the section modulus of the beam. The thickness of mat t should be adequate to withstand maximum shear V (Eq. (9)) experienced by the mat. That means, the mat shear stress F_v must be less than maximum allowable shear stress F_{av} (60 % of the yield strength for steel and aluminum) as given in Eq. (10).

$$V = (qB)L_c \tag{9}$$

$$F_v = \frac{1.5V}{Bt} \tag{10}$$

With the thickness fixed, the final bearing stress needs be checked against the bearing capacity, considering the total payload ($P + P_W$) from Eq. (11).

$$q = \frac{P + P_W}{L_{eff}B} \leq q_a \tag{11}$$

Also, there should be a final check for the deflection Δ using Eq. (12). The deflection limit of 0.75 % of L_c is suggested, where E is the modulus of elasticity of the mat material. Also, the L_{eff} should be less than or equal to ($2L_{cr} + C$) as given in Eq. (13). Here, L_{cr} represents half the distance between the inner edges of crane track chains (Fig. 1).

$$\Delta = \frac{(qB)(L_c)^4}{8EI} \tag{12}$$

$$L_{eff} \leq 2L_{cr} + C \tag{13}$$

The following steps are to be followed for mat design:

Step 1: Define the total lift load P, which is a combination of loads like lifting load, crane counterweight, and crane self-load.

Step 2: Calculate the initial mat effective length L_{eff} (use round-up value) considering the allowable ground bearing pressure $q_a = \frac{q_g}{FS}$ and the lift load P (Eq. (3)).

Step 3: Calculate the actual bearing pressure q under the mat (Eq. (4)).

Step 4: Estimate the thickness t (use round-up value) of the mat (Eq. (8)).

Step 5: Calculate the shear stress F_v on the mat (Eq. (10)).

Step 6: Calculate the actual bearing pressure on the mat q (Eq. (11)).

Step 7: Perform checks as follows:

- Check 1: The actual bearing pressure on the mat q (Eq. (11)) considering total load (including the mat weight W), which should be less than soil allowable bearing capacity q_a.
- Check 2: The shear stress on the mat F_v should be less than the allowable shear stress Fva (60 % of Fy)
- Check 3: The mat edge deflection Δ (Eq. (12)) should be less than the allowable limit (0.75 % of L_{eff})
- Check 4: The mat's effective length should be less than the allowable limit as per Eq. (13).

Step 8: Repeat:

- If the design fails for check 1, increase the effective length L_{eff} and repeat from step 3.
- If the design fails for check 2, increase the mat thickness t and repeat from step 5.
- If the design fails for check 3, increase the mat thickness t and repeat from step 5.
- If the design fails for check 4, the mat material should be changed.

Step 9: If all checks pass, accept the mat design dimensions: effective length, L_{eff} and thickness, t.

3.2. *Mat layout design for transit in field*

Making a mat layout plan for a crawler crane to transit is to find the optimum path that yields the most economical solution for the crane operation. The objective function encompasses minimizing the transit cost *TC* of the crawler crane with heavy weight and, at the same time, minimizing the mat material cost *MC*. Therefore, the total cost of crane transit operation would be,

$$OC = TC + MC \tag{14}$$

To plan the crane transit operation, the first step is to represent the whole site into rectangular grids in a local coordinate system $G(x, y)$ where grid lines are equally spaced (d) in both directions, as shown in Fig. 2.

Once the starting point S and final destination point F of the crane transit are identified, a proper optimization algorithm would be instrumental in finding the shortest distance to transit from S to F. It is important to note that the crane has three degrees of freedom in the defined grid system and can move horizontally, vertically, and diagonally. Each cell in the grid $G(x, y)$ has a weight representing the cost to move through that cell. The cost is calculated based on the mat material cost *MC* and crane transit cost *TC* to traverse from one point to another in the grid system G. Say $G_1(x_1, y_1)$ and $G_2(x_2, y_2)$ are two adjacent cells (Fig. 2), to move from $G_1(x_1, y_1)$ to $G_2(x_2, y_2)$, the crane must transit a distance d'. If G_1 and G_2 are positioned vertically, the transit distance $d' = d$, and if G_1 and G_2 are diagonally positioned, the transit distance $d' = d\sqrt{2}$. For the mat material cost calculation, between the two cells, whichever has the larger dimension and thickness dominates the design and therefore is chosen, and the cost is calculated accordingly. Hence, material cost *MC* derived from the mat material cost per unit length *mc* for the crane to transit from G_1 to G_2 is,

$$MC_{G_1,G_2} = Max\left(mc_{G_1}, mc_{G_2}\right) \times d' \tag{15}$$

Here, $mc_{(x,y)}$ represents the mat material cost at grid coordinate $G(x, y)$, which can be derived from the incurred costs associated with the purchase or rental of mat material. The required volume of mat material V_m per unit length is given by $V_m = \left(L_{eff} \times t \times 1\right)$, while the crane is traveling a distance d' from one node of the grid system to node G. Similarly, if crane operation cost for traveling per unit length of travel distance is *tc,* transit operation cost for the crane to travel from $G_1(x_1, y_1)$ to $G_2(x_2, y_2)$ is,

$$TC_{G_1,G_2} = tc_{G_1,G_2} \times d' \tag{16}$$

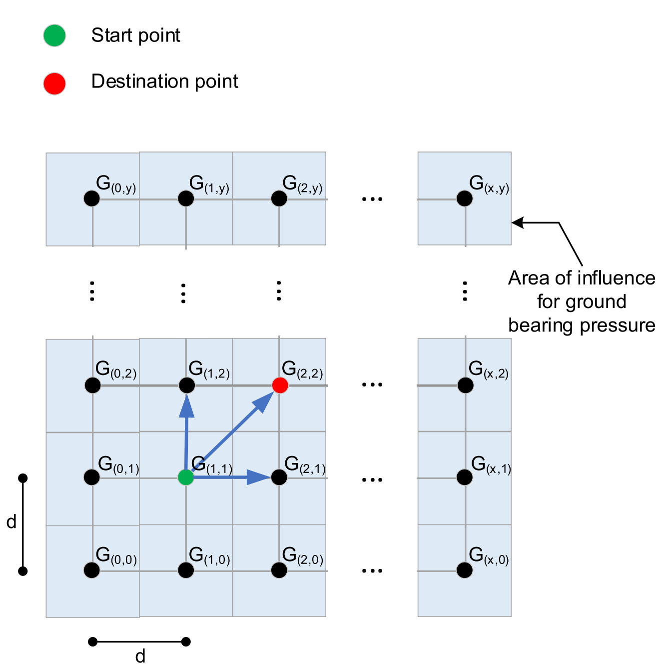

Fig. 2. Construction site layout in the form of a grid system.

Now, the crane transit cost is directly proportional to crane operational speed, which is influenced by the ground profile (elevation/contour). For instance, when a crane moves on a slope, the speed must be reduced to ensure safe transit and prevent tipping hazards due to the imbalance of the center of gravity and sudden momentum changes [45]. It is noteworthy that speed limitations on slopes are often dictated by Occupational Health and Safety (OHS) codes or lift design standards relevant to particular jurisdictions; one such example is the Alberta Occupational Health and Safety Code [46]. If the slope between grids $\alpha = \frac{\Delta_{G_1,G_2}}{d'}$ (where Δ_{G_1,G_2} is the elevation difference and d' between two grid locations G_1 and G_2) exceeds a certain limit α^o, movement over such a ground profile is generally prohibited. Note that in the case of Alberta, Canada, crane movement must comply with the Alberta Occupational Health and Safety Code [46], which also references the Canadian Standard Association Code Z150:20 [47]. Consequently, crane operation speed may vary along the transit path, impacting the overall operational cost. Therefore, the crane operation cost for transit per unit length of transit distance is *tc* as denoted in the Eq. (17), where *v* is the crane transit speed from $G_1(x_1, y_1)$ to $G_2(x_2, y_2)$ and *tc'* is the crane operation cost per unit time of operation.

$$tc_{(1,1),(2,2)} = \begin{cases} \infty;\ \text{for } \alpha > \alpha^o \\ \dfrac{tc'_{G_1,G_2}}{v_{G_1,G_2}};\ \text{for } \alpha \le \alpha^o \end{cases} \tag{17}$$

Therefore, for these two points, the total cost of crane operation cost *OC* can be found from Eq. (18), where *oc* is the crane operation cost per unit transit length of the crane.

$$OC_{G_1,G_2} = TC_{G_1,G_2} + MC_{G_1,G_2}$$

$$OC_{G_1,G_2} = \left(Max\left(mc_{G_1,G_2}, mc_{G_1,G_2}\right) + tc_{G_1,G_2}\right) \times d' = oc_{G_1,G_2} \times d' \tag{18}$$

Hence, the optimization function for crane transit operations can be expressed as shown in Eq. (19), which effectively identifies the least-cost path from the starting point to the finishing point.

$$OC_{G_S,G_F} = min_{p \in Pa}\left(\left(OC_{G_S,G_F}\right)^p\right) \tag{19}$$

Here, *Pa* is the set of all possible paths from G_S to G_F, and $\left(OC_{G_S,G_F}\right)^p$ represents the cost of a particular path *p* from G_S to G_F.

3.3. Dijkstra's graph search algorithm for crane mat layout planning

To solve the problem of crane path planning, which means finding the most economical path for the crane to transit from start point *S* to the destination point *D*, Dijkstra's graph is used. Dijkstra's algorithm is cost effective for computing the shortest path in weighted graphs. Dijkstra's graph search algorithm identifies the shortest path between two nodes in a graph by iteratively exploring paths from the source node to the target node [48]. For each new node discovered, the shortest path to the destination node is fixed using the currently known distances. The following are the steps to follow to run the Dijkstra's algorithm:

Step 1: Initialization: Start by assigning a tentative distance value to every node in the graph $G(x,y)$:

- The distance D to the starting node *S* is set to zero because it's the starting point: $D(S) = 0$.
- The distance to all other nodes *V* is set to infinity: $(V) = \infty$. This signifies that the nodes are initially unreachable.
- Initially, all nodes are placed into an unvisited set *Q*.

Step 2: Current Node Selection:

- Select the unvisited node *U* with the smallest tentative distance $D(U)$ from *Q*. This node becomes the current node.

Step 3: Neighbor Evaluation:

- For the current node U, examine each of its neighbors V (nodes that can be reached directly from the current node).
- Calculate the tentative distance to each neighbor V: the new distance,

$$D(V) = D(U) + W(U, V) \tag{20}$$

Where, $W(U, V)$ is the weight of the move from U to V. In this paper, $W(U, V)$ represents the total minimum operations cost (OC) of the crane, where OC is calculated as per Eq 18. In $W(U, V)$, U denotes the cumulative OC for traversing all previous points along the crane's transit path, V is for the current minimum OC in moving from U to V.

$$W(U, V) = W(U, OC_V) = W(U, (oc_V \times d^{'})) \tag{21}$$

- Take the smallest distance among all the currently known distances to the neighbor as the neighbor's distance and select that node as part of the travel path via selecting the minimum distance using Eq. (22).

$$D(V) = Min(D(V)_i) \tag{22}$$

Where, i is the number of neighbors.
Step 4: Mark as Visited:

- After evaluating all the neighbors of the current node U, mark U as visited and remove U from the unvisited set Q.

Step 5: Repeat:

- Repeat steps 2–4 until all nodes in Q have been visited or until the destination node F is reached.

Step 6: Completion:

- The algorithm terminates when all nodes are visited or when the shortest path to the destination node F is found.
- The shortest path from the starting node S to the destination node F is determined by the recorded distances $D(V)$.

Step 7: Path Construction:

- To trace the shortest path, follow the nodes with the smallest recorded distances from F back to S.

3.4. Example application case of crane transit path planning

Suppose there is a graph representing a grid with six nodes: S, B, C, D, E, and F; the operation cost for each node is 0, 2, 3, 5, 4, and 4 respectively as shown in Fig. 3. The horizontal spacing between gridlines is 3, and the vertical spacing is 4. The start node in the site is S and the destination node is F.

Step 1 – Initialization: Since a is the start node ($a = S$) and f is the finish node ($f = F$). Here, $D(a) = 0$, and $D(b) = D(c) = D(d) = D(e) = D(f) = \infty$. The unvisited set $Q = \{a, b, c, d, e, f\}$.

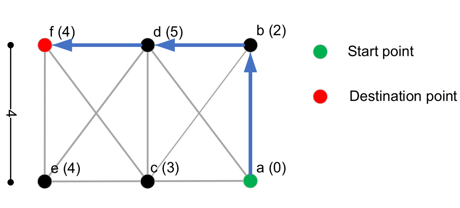

Fig. 3. Construction site layout of the example case.

Step 2 – Current Node Selection: Select node S because it has the smallest distance (0) in the Q.

Step 3 – Neighbor Evaluation: Neighbors of a are b, c, and d. Therefore form,

$$D(b) = min(\infty, (0 + 2) \times 4) = 8$$

$$D(c) = min(\infty, (0 + 3) \times 3) = 9$$

$$D(d) = min(\infty, (0 + 5) \times 5) = 25$$

Step 4 – Mark as Visited: Mark a as visited and remove it from Q.
Step 5 – Repeat:

- Next, select node b because it has the smallest distance (8). The neighbors of b are c and d.

$$D(c) = min(9, 8 + 3 \times 5) = 23$$

$$D(d) = min(25, 8 + 5 \times 3) = 23$$

- Next, select node c, d because it has the smallest distance (23), so both are eliminated form Q. Let's select c and the neighbors of c are, e and f.

$$D(e) = min(\infty, 23 + 4 \times 3) = 35$$

$$D(f) = min(\infty, 23 + 4 \times 5) = 43$$

- Select d and the neighbors of d are, e and f

$$D(e) = min(\infty, 23 + 4 \times 5) = 43$$

$$D(f) = min(\infty, 23 + 4 \times 3) = 35$$

- Both e, f are visited and removed from Q.
- Since f is reached from d, d is in the path from S to F.

Step 6 – Completion: The destination node is reachd; therefore, the program terminates.

Step 7 – Path Construction: The path to transit form S to F is $a \to b \to d \to f$.

4. Crane transit path planning methodology: Application framework

In this research, engineering design of crawler crane mats is integrated with graph search algorithms to enrich the crane transit path planning optimization problem. The entire crane transit path planning methodology is divided into two stages: 1) initialization of design parameters, and 2) formulation of crane mat layout plans, as elaborated below.

4.1. Initialization of design parameters

- The process begins by dividing the site into a grid system G(x,y), with the grid size (d) determined by the variability in soil bearing capacity. Given the high subsurface variability between adjacent grids (e.g., above 15 kPa), a finer grid is recommended. Conversely, if the variability is negligible (e.g., below 5 kPa), a larger grid size is sufficient.
- Within the grid system G(x,y), the next step is to identify the coordinates of the crane's starting point (S) and destination (F), along with any inaccessible areas (X). Inaccessible regions may include existing site infrastructure, areas occupied by other construction

activities, or zones deemed unsafe for crane operation (e.g., steep slopes or collision risks.)

- In the grid system, soil bearing capacity (q_g) values are assigned to each node based on site soil geotechnical investigations. If measurements are unavailable for some locations, values are interpolated using the lowest bearing capacity between adjacent points to ensure safety.
- Additionally, mapping site slopes is critical for safe and efficient crane operations. According to IHSA [49], slope exceeding 3 % is generally considered unsafe (also depending on the crane's payload and boom angle); while slope less than 1 % gradient is ideal.

4.2. Formulation of crane mat layout plans

- With the information outlined, follow the methods described in Section 3.1 to determine the required width and thickness of the crane mats between grid nodes. This procedure is applied to all possible node combinations.
- Next, the operational cost (OC) of crane transit is calculated, considering the mat material cost (MC) based on the mats design performed in the previous step and the crane transit cost (TC) depending on operating speed and travel distance, as elaborated in Section 3.2, Eqs. (15) & (16).
- Subsequently, a weight (W) is associated with the linkage between grid nodes denoting OC (determined as per Eq. (18)), essential for identifying the least-cost path for crane operations. It is notable that if the transit gradient exceeds a safety threshold, crane operation would become unsafe, and hence the operational cost is set to infinity (Eq. (17)). The overall objective of crane mat layout planning optimization is to minimize total OC, as expressed in Eq. (19).
- With weights assigned throughout the site grid system, Dijkstra's Algorithm, described in Section 3.3, is effectively applied to derive the optimal crane mat layout.

The framework for applying the proposed methodology is illustrated in Fig. 4.

The next section of this paper presents a case study to demonstrate the step-by-step application of the proposed methodology. Based on a real-world construction project, the case study provides sufficient details to illustrate practical implementation of the method. The approach offers a systematic framework with defined input parameters and optimized solutions. Before field deployment, the solution can be effectively communicated to site operations personnel through graphical representations and validated by comparing its total cost to solutions derived from heuristics or based on experience under the same input conditions.

5. Case study

5.1. General information

A stadium construction case is used to demonstrate the practical application of the proposed method for crane operation layout planning. Note the case is based on a real-world project which was originally investigated for demonstrating the implementation of discrete-event simulation for construction operations planning [11], which provides the basis for this current case study and is further adapted by assuming the information on the soil bearing capacity in the field and site surface profile information (such data was not available in the original case publication). The stadium occupies an area of 258,000 square meters, with a giant steel latticework serving as the outer frame, covering bowl-shaped concrete structures (gallery), as shown in Fig. 5. The roof framework is supported by twenty-four steel columns situated around the grandstand. These steel columns are substantial structures, with heights varying from 40 m to 69 m, consisting of many steel elements. All structural column elements were fabricated in a remote fabrication shop and hauled to the construction site storage area adjacent to the assembly yard for installation. The prefabricated components are assembled in the yard and then transported to the designated location for erection using a crawler crane. The columns are assembled into two separate modules, referred to as the lower portion and the upper portion. The weight of the columns varied from 110 tons to 140 tons.

In the actual construction field, the assembly yards were strategically located at the boundary of the main construction site to provide designated site access points. This placement allowed for the efficient movement of prefabricated components from the fabrication shop to the sites without incurring extra traffic. Additionally, the assembly yards were established at a sufficient distance from the primary construction zones to minimize site congestion. This spatial arrangement facilitated smoother logistics and uninterrupted movement of materials and personnel, significantly enhancing the overall efficiency and safety of

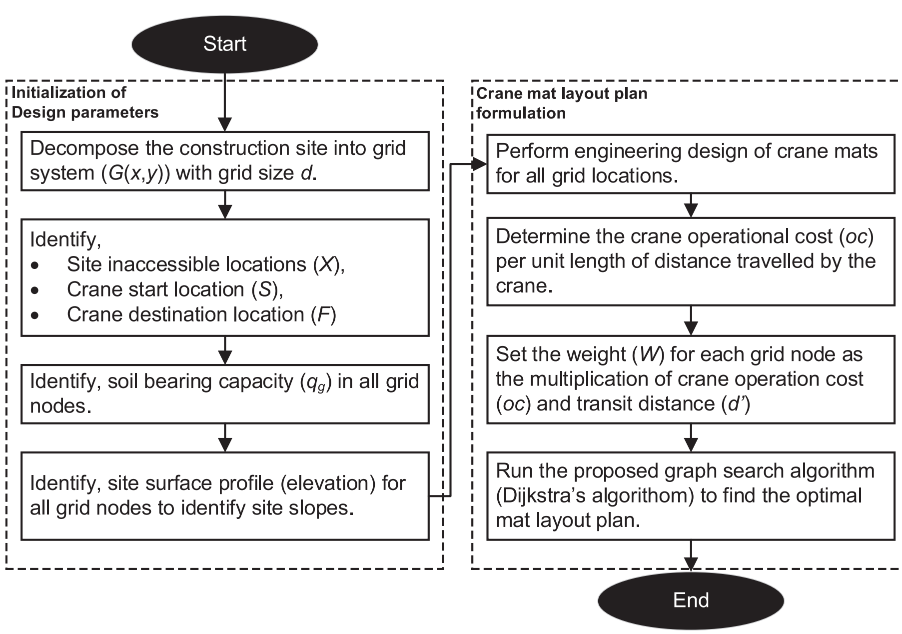

Fig. 4. Application framework for preparing crane mat layout plan (crane transit path plan).

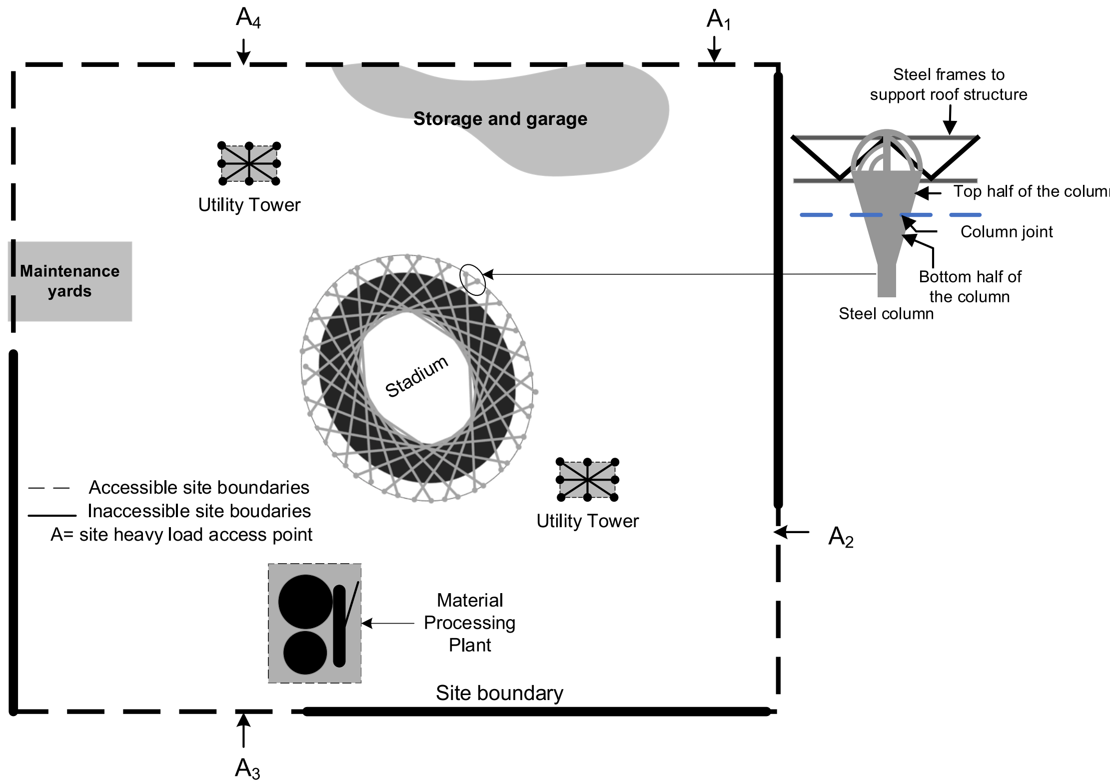

Fig. 5. Sketch of the stadium construction site for the case study project.

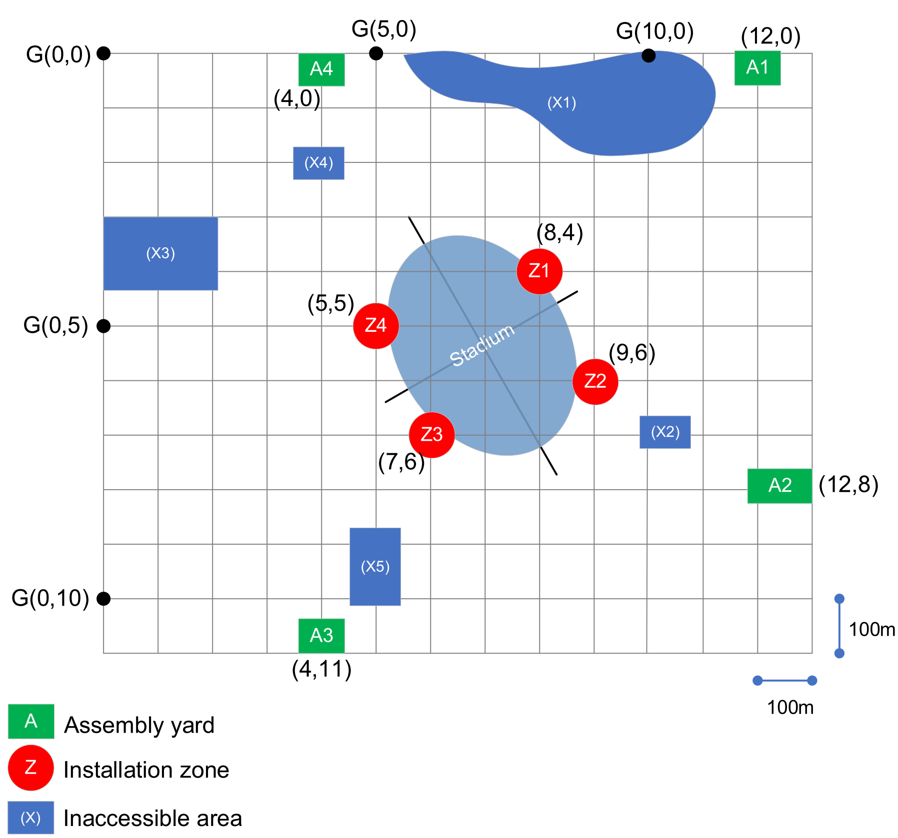

Fig. 6. Schematic of the construction site with various site elements identified in the grid system.

the construction operations. The fully loaded crawler crane moved slowly along temporary steel mats from the site assembly yard to the designated installation spot. The process was carefully controlled by the site crew. Upon completion of the installation, the crawler crane returned to the designated assembling area for the next lift in accordance with the planned column erection sequence and the structure construction sequence (the lower portion should be erected prior to the upper portion, followed by the installation of top frames). The schematic of the site layout is provided in Fig. 6.

5.2. Method application: plan formulation

To perform the planning exercise, first the entire site is divided into virtual grids, with grid lines spaced 100 m apart in both X and Y directions, considering the size of the stadium construction site. It is notable that the grid width depends on the variation in ground soil bearing capacity in the field resulting from initial geotechnical investigations: the higher variation leads to finer cells. In the current case, the ground bearing pressure at different grid locations is assumed to be known (Fig. 6). Generally, soil investigations are performed at intervals of 200 m, and values for the intermediate grid locations are interpolated from the values of the adjacent locations. The lowest value between two adjacent locations is used for the interpolated value of the location. The soil bearing capacities at different locations are presented in Table 1.

Note, for a typical site with relatively homogeneous subsurface condition (e.g., the original ground), the variations in soil properties along the depth for geotechnical investigation are rather insignificant in the site area. On the other hand, where the site is on the fill ground consisting of excavated soils from various cut sources, variations in soil properties become considerable. The general practice for crane mat design and heavy lift planning is to take the most unfavorable soil from limited bore hole samples in the coverage area. Obviously, in the latter case, the grid size needs to decrease (e.g., 50 m) so as to allow sufficient subsurface mapping. It is worth mentioning that the grid size is taken as a model parameter of the proposed optimization method, which is subject to adjustment to the application needs. The crane transits between equally spaced grid nodes, moving either in straight lines or diagonally. The soil bearing capacity and ground elevation at each node are predetermined inputs. Note that in order to ensure stability and safety of the crane operations, the crane is only allowed to move between nodes at a safe speed on the transit path laid with mats of specified length and thickness.

A crawler crane (MAMMOET Demag CC 4800; rated maximum load capacity 800 ton) is deployed to transport and install all the columns. The crane mats are designed based on the soil-bearing pressure at grid locations and the maximum weight of the column modules, which is 140 tons for the bottom, top, and frame sections, following the mat design method presented in Section 3.1. The crane is continuously engaged in the lifting, transporting, and installing of twenty-four column units and forty-three frame units, with no idling or downtime except for maintenance and repair. The crane transits at an average speed of 50 m per hour when fully loaded and 100 m per hour when empty on return trips on the flat surface ($\alpha = 0$). The crane operating speed decreases by 10 % for a 0.3 % slope change, and the crane stops operating when the ground slope is more than 3 % ($\alpha^o = 0.03$). Note the site elevations at each grid for the case study are assumed (shown in Table 2) as the actual data were not available in the original case.

A detailed crane transit plan is essential for coordinating with other site logistics activities and ensuring operations safety. For this case study, the hourly crane operation cost is assumed at $22,500, which includes the crane rental, crew operation cost, logistics, and delay/interruption costs to other operations due to the crane's movement. In addition, $13,000 per cubic meter of mat is considered when calculating the material cost. Note those rates do not represent the actual values, only facilitating the calculation of the cost function in optimization in the current case study. Table 3 summarizes the input parameters for finding the crane mat design and calculating the mat material cost *mc(x, y)* per unit length. Combining *mc(x,y)* with crane transit cost *tc(x,y)*per unit length, weights assigned to each grid coordinate are determined for use in the graph search algorithm for crane path planning. It is important to note that the mat rental cost for predetermined sizes can be determined by the unit rate and the quantity of particular mats. In practice, the rental cost can be quoted as a lump sum; but from the business point of view, a breakdown of unit rate and quantity for a specific type of mat is more appropriate; while the unit rate of mat also depends on the condition of the mat (wear and tear) and the number of times the mat has been used. This is analogous to estimating the formwork cost for repeated use in concreting building components in terms of made assumptions and calculation logic. Additionally, the proposed method provides the minimum size requirements for the mat, which can be easily converted to the quantity of standard-sized mats needed. This, in turn, facilitates the calculation of rental costs.

The soil bearing capacity values for all grid locations are assumed in the case study, as shown in Table 4 and corresponding engineering design details for the crane mats are calculated using the mat design method described in Section 3.2 are given in Table 5.

The engineering design information of mats for each coordinate location is subsequently utilized to calculate the crane operation costs (*oc*) per unit length of crane movement. Note this calculation combines the crane mat material cost with the movement cost per unit transit length, dependent on the crane's hourly operation cost and transit speed. The crane operation costs (*oc*) for each coordinate are summarized in Table 6. These values, when multiplied by the transit distance d' (Eq. (19)), are used as nonnegative weights for the graph search algorithm in optimizing the crane mat layout planning problem. All weight input values (*w*) are provided in Table 7. For a few coordinates, as shown in Table 7, the *w* values are set to "∞" artificially to define inaccessible areas.

With all the coordinate weights (*w*) set and all assembly stations and installation locations identified (start coordinates: (12,0), (12,8), (4,11), (4,0) and corresponding end coordinates: (8,4), (9,6), (6,7), (5,5) respectively), the crane mat layout (transit path) planning was executed to formulate the crane mat layout plan (as per Section 3.3). The obtained results of the optimum crane transit paths are as follows, which are also illustrated in Fig. 7:

- Path 1 - from assembly area A1 to installation zone Z1: G[(12,0), (12,1), (11,2), (10,2), (9, 3), (8, 4)]
- Path 2 - from assembly area A2 to installation zone Z2: G[(12, 8), (11, 9), (10, 8), (9, 7), (9, 6)]
- Path 3 - from assembly area A3 to installation zone Z3: G[(4, 11), (5, 11), (6, 11), (6, 10), (6, 9), (6, 8), (6, 7)]
- Path 4 - from assembly area A4 to installation zone Z4: G[(4, 0), (3,1), (3,2), (3,3), (4, 4), (5, 5)]

Table 1
Ground bearing pressure at different site grid locations.

	Soil allowable bearing capacity q_a (kPa)							
		x coordinates in the grid system G						
	G (x, y)	**1**	**3**	**5**	**7**	**9**	**11**	**13**
y coordinates in the grid system G	**1**	95	145	145	85	85	115	115
	3	100	150	90	90	115	115	155
	5	80	80	135	135	85	85	90
	7	140	100	100	140	155	85	85
	9	150	95	95	155	160	165	165
	11	120	120	170	115	110	110	110

Table 2
Site ground profile.

	Elevation of the ground from the datum (m)														
			x coordinates in the grid system G												
	G(x,y)	**0**	**1**	**2**	**3**	**4**	**5**	**6**	**7**	**8**	**9**	**10**	**11**	**12**	**13**
y coordinates in the grid system G	**0**	0	0	0	4	3	0	∞	∞	∞	∞	∞	4	4	2
	1	2	4	4	4	1	1	∞	∞	∞	∞	∞	∞	4	2
	2	4	4	4	4	3	2	4	4	4	4	4	4	2	3
	3	∞	∞	∞	4	4	3	4	4	4	4	2	4	3	4
	4	∞	∞	∞	4	4	4	4	4	4	3	4	4	4	4
	5	4	4	4	4	4	4	4	4	4	4	3	4	3	4
	6	4	4	4	4	4	4	4	4	4	4	4	4	3	2
	7	4	4	3	4	4	4	4	4	4	4	∞	3	2	2
	8	4	4	2	1	1	3	4	4	4	4	4	3	3	3
	9	4	4	3	2	2	∞	4	4	4	4	4	3	2	3
	10	4	4	4	4	4	∞	4	4	4	4	3	4	4	4
	11	4	4	4	4	4	4	4	4	4	4	4	4	4	4

Table 3
Input parameters for crane mat design.

Description	Variable	Value
Total lift load	*P1*	140 ton
Crane weight	*P2*	20 ton
Counterweight	*P3*	200 ton
Soil ultimate bearing capacity	q_g	145 kPa
Factor of safety (to find q_a from q_g)	*FS*	2
Width of the crawler crane chain	*C*	1.5 m
Distance between two crawler crane chains (outer edge	L_{cr}	12 m
Length of the crawler crane chain	*B*	12.57 m
Yield strength of the mat plate for A36 steel plates	F_y	250 Mpa
Modulus of elasticity of steel	*E*	200 Gpa

5.3. Plan analysis

The crane mat plan generated by the proposed algorithm is compared with a plan considering only the shortest transit distances from the assembly yard to the column/frame installation zones. Notably, practitioners intuitively rely on similar rules of thumb in planning for the crane paths. As illustrated in Fig. 8, the shortest path plans are:

- Path 1 - from assembly area A1 to installation zone Z1: G[(12, 0), (12, 1), (11, 2), (10,3), (9, 4), (8, 4)]
- Path 2 - from assembly area A1 to installation zone Z1: G[(12, 8), (11, 7), (10, 6), (9, 6)]
- Path 3 - from assembly area A1 to installation zone Z1: G[(4, 11), (4, 10), (4, 9), (5, 8), (6, 7)]
- Path 4 - from assembly area A1 to installation zone Z1: G[(4, 0), (4, 1), (5, 2), (5, 3), (5, 4), (5, 5)]

In the current case study, a cost analysis was conducted to compare the cost of moving through the crane mat layout developed using the proposed method against the cost of the geometrically shortest path. The developed graph search algorithm was run with uniform coordinate weights ($w = 1$) for all the coordinates. The comparisons are illustrated in Fig. 9. On all the paths (Path 1 to Path 4), the crane mat layout plan algorithm developed is found to be more cost-efficient, resulting in lower costs. In this case study, results from the proposed method averages approximately a 33 % cost saving per lift job from assembly yards to installation zones.

It is worth mentioning that the workability of the proposed plan can be verified by systematically following the analytical method step by step and cross-examining the optimized solution. It is stressed that the optimum solution as obtained acts as decision support to the site engineer or the construction manager, who can easily perform independent checks on the mats design along the recommended crane transit path in order to assure the workability of the solution prior to implementation in field.

5.4. Influence of different grid size in mat layout plan

In the previous section, a methodology is developed to synchronize the crane mat design with the mat layout plan. Building on this methodology, the present section examines the impact of grid size on crane mat planning. The developed algorithm is employed to evaluate the influence of grid size on the planning layout. To apply the method with different grid sizes, it is sufficient to identify the coordinates of relevant points on the site with the new grid size imposed. Three additional grid sizes are assessed, namely: 50 m, 25 m, and 12.5 m. Critical locations and constraints on the site, including the start and destination points for

Table 4
Estimated bearing capacity at different site coordinates.

	Soil allowable bearing capacity q_a (kPa)														
			x coordinates in the grid system G												
	G(x,y)	0	1	2	3	4	5	6	7	8	9	10	11	12	13
y coordinates in the grid system G	***0***	95	95	155	135	135	135	160	85	85	85	140	115	115	115
	1	95	95	155	145	145	145	160	85	85	85	140	115	115	115
	2	95	95	155	140	140	90	90	85	85	85	115	115	115	115
	3	100	100	155	150	150	90	90	90	145	115	115	115	155	155
	4	100	80	80	80	135	110	110	110	135	85	85	85	90	90
	5	105	80	80	80	135	135	150	135	135	85	85	85	90	90
	6	105	80	80	80	100	100	140	135	135	85	85	85	85	85
	7	140	140	140	100	100	100	140	140	155	155	155	85	85	85
	8	140	140	140	95	95	95	140	140	155	155	155	85	85	85
	9	150	150	150	95	95	95	155	155	160	160	165	165	165	165
	10	150	120	120	95	95	95	155	115	115	110	110	110	110	110
	11	145	120	120	120	170	170	170	115	115	110	110	110	110	110

Table 5
Mat dimensions for different site coordinates as per the soil bearing capacity given in Table 4.

	Designed Mat (Length (m), Thickness (mm))														
			x coordinates in the grid system G												
	G(x,y)	0	1	2	3	4	5	6	7	8	9	10	11	12	13
y coordinates in the grid system G	**0**	(6.75,85)	(6.75,85)	(4,55)	(4.5,60)	(4.5,60)	(4.5,60)	(4,55)	(7.75,90)	(7.75,90)	(7.75,90)	(4.25,55)	(5.5,70)	(5.5,70)	(5.5,70)
	1	(6.75,85)	(6.75,85)	(4,55)	(4.25,55)	(4.25,55)	(4.25,55)	(4,55)	(7.75,90)	(7.75,90)	(7.75,90)	(4.25,55)	(5.5,70)	(5.5,70)	(5.5,70)
	2	(6.75,85)	(6.75,85)	(4,55)	(4.25,55)	(4.25,55)	(7.25,90)	(7.25,90)	(7.75,90)	(7.75,90)	(7.75,90)	(5.5,70)	(5.5,70)	(5.5,70)	(5.5,70)
	3	(6.5,80)	(6.5,80)	(4,55)	(4,55)	(4,55)	(7.25,90)	(7.25,90)	(7.25,90)	(4.25,55)	(5.5,70)	(5.5,70)	(5.5,70)	(4,55)	(4,55)
	4	(6.5,80)	(8.5100)	(8.5100)	(8.5100)	(4.5,60)	(5.75,75)	(5.75,75)	(5.75,75)	(4.5,60)	(7.75,90)	(7.75,90)	(7.75,90)	(7.25,90)	(7.25,90)
	5	(6,75)	(8.5100)	(8.5100)	(8.5100)	(4.5,60)	(4.5,60)	(4,55)	(4.5,60)	(4.5,60)	(7.75,90)	(7.75,90)	(7.75,90)	(7.25,90)	(7.25,90)
	6	(6,75)	(8.5100)	(8.5100)	(8.5100)	(6.5,80)	(6.5,80)	(4.25,55)	(4.5,60)	(4.5,60)	(7.75,90)	(7.75,90)	(7.75,90)	(7.75,90)	(7.75,90)
	7	(4.25,55)	(4.25,55)	(4.25,55)	(6.5,80)	(6.5,80)	(6.5,80)	(4.25,55)	(4.25,55)	(4,55)	(4,55)	(4,55)	(7.75,90)	(7.75,90)	(7.75,90)
	8	(4.25,55)	(4.25,55)	(4.25,55)	(6.75,85)	(6.75,85)	(6.75,85)	(4.25,55)	(4.25,55)	(4,55)	(4,55)	(4,55)	(7.75,90)	(7.75,90)	(7.75,90)
	9	(4,55)	(4,55)	(4,55)	(6.75,85)	(6.75,85)	(6.75,85)	(4,55)	(4,55)	(4,55)	(4,55)	(3.75,50)	(3.75,50)	(3.75,50)	(3.75,50)
	10	(4,55)	(5.25,70)	(5.25,70)	(6.75,85)	(6.75,85)	(6.75,85)	(4,55)	(5.5,70)	(5.5,70)	(5.75,75)	(5.75,75)	(5.75,75)	(5.75,75)	(5.75,75)
	11	(4.25,55)	(5.25,70)	(5.25,70)	(5.25,70)	(3.5,45)	(3.5,45)	(3.5,45)	(5.5,70)	(5.5,70)	(5.75,75)	(5.75,75)	(5.75,75)	(5.75,75)	(5.75,75)

cranes and inaccessible areas, are considered. The soil geotechnical properties for the new grids are conservatively interpolated (selecting the lowest value of the soil bearing capacity from a set of values during interpolation). In practice, practitioners may conduct additional borehole investigations to confirm the assumptions, considering the trade-off between the cost of soil investigation, potential delays, and possible final savings. Two tables in the appendix, namely, Tables A1 and A2 summarize the planning results obtained using the shortest path algorithm and the proposed algorithm, respectively. Notably, the proposed path planning algorithm yields a more efficient plan, providing cost savings ranging from 13 % to 21 % compared to the shortest path plan across all grid sizes being assessed.

The cost of crane transit operations, plotted in Fig. 10, gradually decreases as the grid size reduces from 100 m to 25 m and slightly increases when the grid size is further reduced to 12.5 m. This suggests an opportunity to refine the results using heuristics (e.g., the bisection method) to set up the grid size, considering the potential savings from smaller grid sizes, the availability of mat model sizes in the market, and the ease of setup and customization [50].

Considering this case study, the 25 m × 25 m grid size yields the best result and is recommended for implementation. In addition, a new optimization problem emerges: how to decide on the optimal grid size using mathematical optimization or heuristics algorithms. Nonetheless, this is beyond the scope of this research and will be left for future work. Based on the proposed plan, the project manager or construction planner can determine the number of mats required for their respective sizes. The proposed plan with the 25 m × 25 m grid size is shown on Fig. A1 and summarized in Table A2.

Assuming the manufacturer produces mats with a 2.5 m width, the following table (Table 8) gives the number of mats required for the job, along with the total travel length and mat sizes needed according to the plan generated by the proposed methodology. The mat sizes used in an actual job can either be custom-made or adjusted by the construction planner based on market availability. When selecting the manufacturer's ready-made mats, it is advisable to choose mats with a size larger than the one recommended in the plan and perform an additional check of design adequacy using the method presented in Section 3.1. Table 8 summarizes the number of mats required for the planned job, with an additional 5 % cushion factored in to account for potential sizing issues in the field.

6. Conclusion

The research described in this paper focused on optimizing crane mat design and transit path layout planning, an area that had been previously underexplored and under-researched but became increasingly significant as the technology of offsite prefabrication and modular construction advanced rapidly. An approach was developed using graph search algorithms to optimize crane mat design and transit path planning. This method accounted for both the shortest travel distances and the mats material and crane movement costs, resulting in more efficient and cost-effective solutions.

Ensuring adequate ground bearing capacity and implementing a well-designed mat layout plan can significantly enhance operational safety and efficiency. This research represents the first attempt to consider the ground profiles of a construction site, namely: the geotechnical profile (bearing capacity) and the surface profile (slopes) in devising the optimization method for planning the mat size and layout for stable and safe operations of the crane. The introduction of an automated mat layout optimization algorithm would lead to a significant advancement of the current practice, reducing preparation time and minimizing the need for manual revisions. This innovation holds the potential for improving the planning and execution of crane operations in modular construction projects as well as industrial and infrastructure construction projects involving prefabrication and installation of large and heavy structural components. It is noteworthy that the proposed

Table 6
Crane operational cost used as the weight for crane path planning.

	Crane operational cost per meter transit length, $oc_{i,j}$ ($/per meter length)														
			x coordinates in the grid system *G*												
	G(*x*,*y*)	0	*1*	2	*3*	4	*5*	6	*7*	8	*9*	10	*11*	12	*13*
y coordinates in the grid system G	0	7684	7684	3085	3735	3735	3735	3085	9293	9293	9293	3264	5230	5230	5230
	1	7684	7684	3085	3264	3264	3264	3085	9293	9293	9293	3264	5230	5230	5230
	2	7684	7684	3085	3264	3264	8708	8708	9293	9293	9293	5230	5230	5230	5230
	3	6985	6985	3085	3085	3085	8708	8708	8708	3264	5230	5230	5230	3085	3085
	4	6985	11,275	11,275	11,275	3735	5831	5831	5831	3735	9293	9293	9293	8708	8708
	5	6075	11,275	11,275	11,275	3735	3735	3085	3735	3735	9293	9293	9293	8708	8708
	6	6075	11,275	11,275	11,275	6985	6985	3264	3735	3735	9293	9293	9293	9293	9293
	7	3264	3264	3264	6985	6985	6985	3264	3264	3085	3085	3085	9293	9293	9293
	8	3264	3264	3264	7684	7684	7684	3264	3264	3085	3085	3085	9293	9293	9293
	9	3085	3085	3085	7684	7684	7684	3085	3085	3085	3085	2663	2663	2663	2663
	10	3085	5003	5003	7684	7684	7684	3085	5230	5230	5831	5831	5831	5831	5831
	11	3264	5003	5003	5003	2273	2273	2273	5230	5230	5831	5831	5831	5831	5831

Table 7
Nonnegative weights for graph search algorithm for crane path planning.

	w portion of the Nonnegative weight W														
			x coordinates in the grid system *G*												
	G(*x*,*y*)	0	*1*	2	*3*	4	*5*	6	*7*	8	*9*	10	*11*	12	*13*
y coordinates in the grid system G	0	7684	7684	3085	3735	3735	3735	∞	∞	∞	∞	∞	5230	5230	5230
	1	7684	7684	3085	3264	3264	3264	∞	∞	∞	∞	∞	∞	5230	5230
	2	7684	7684	3085	3264	∞	8708	8708	9293	9293	9293	5230	5230	5230	5230
	3	∞	∞	∞	3085	3085	8708	8708	8708	3264	5230	5230	5230	3085	3085
	4	∞	∞	∞	11,275	3735	5831	5831	5831	3735	9293	9293	9293	8708	8708
	5	6075	11,275	11,275	11,275	3735	3735	3085	3735	3735	9293	9293	9293	8708	8708
	6	6075	11,275	11,275	11,275	6985	6985	3264	3735	3735	9293	9293	9293	9293	9293
	7	3264	3264	3264	6985	6985	6985	3264	3264	3085	3085	3085	∞	9293	9293
	8	3264	3264	3264	7684	7684	7684	3264	3264	3085	3085	3085	9293	9293	9293
	9	3085	3085	3085	7684	7684	∞	3085	3085	3085	3085	2663	2663	2663	2663
	10	3085	5003	5003	7684	7684	∞	3085	5230	5230	5831	5831	5831	5831	5831
	11	3264	5003	5003	5003	2273	2273	2273	5230	5230	5831	5831	5831	5831	5831

mat design method is only applicable to steel or aluminum mats that are commonly used on oversized and superheavy lifts in construction, as in the presented case study. On the other hand, crane mats made of timber can also be accommodated with minor modifications in the formulas for mat size checks against shear stress [12].

The findings from the described case study demonstrate a significant improvement in cost efficiency. Approximately 20 % to 30 % cost saving was obtained compared to the general practice that considers only the geometrically shortest path. This reinforces the significance of incorporating comprehensive cost factors into crane mat layout planning as opposed to focusing solely on distance minimization. Furthermore, the application of graph search algorithms in crane mat layout planning lends practical benefits. For instance, the automation of this process would reduce the time and effort required from practitioners, leading to optimum layout plans backed with computing. These optimized plans not only save costs but also contribute to sustainable construction practices by minimizing the quantity of crane mats required, thereby reducing the environmental impact associated with their manufacturing and usage.

It is noteworthy that the research problem is inspired by a real project. However, the case study is based on a project conducted in 2005/06. Due to limitations of project data collected then, additional data for the parameters of the proposed model were made up by making reasonable assumptions in order to prove concept for this research. Given any differences in the actual site or on a new project, those model parameters need to be adjusted to rerun the computer model and update the solutions. The inputs, the algorithmic logic, and the outputs for the proposed research are presented in such a transparent fashion as to allow for manual checking and verification.

One limitation of the proposed crane path design method lies in the fact that deciding the proper grid size in setting up the field for analysis has yet to be addressed in an analytical way. Higher variations in the soil geotechnical profile would necessitate finer grid sizes; this correlation warrants further investigation in the follow-up research. Note that for addressing the crane mat design problem, requirements for penetration depth and test accuracy in field investigation are not high. Mature technology -resulting from recent research for investigating field ground cost-effectively, such as the land survey rover for site surface profile mapping, the remodeled bobcat [51] or portable ground penetration radar [52,53]- can be instrumental in performing site investigation and collecting required data. These advancements will enable timely planning and efficient execution of the proposed new approach, ultimately contributing to safer, more productive, and more sustainable operations of high-capacity crawler cranes in construction fields.

CRediT authorship contribution statement

Monjurul Hasan: Problem statement based on investigating practice and literature, Writing – review & editing, Writing – original draft, Visualization, Validation, Software, Methodology, Investigation, Formal analysis, Data curation, Conceptualization. **Ming Lu:** Problem statement based on investigating practice and literature, Writing – review & editing, Validation, Methodology, Conceptualization.

Declaration of competing interest

The authors declare that they have no known competing financial interests or personal relationships that could have appeared to influence the work reported in this paper

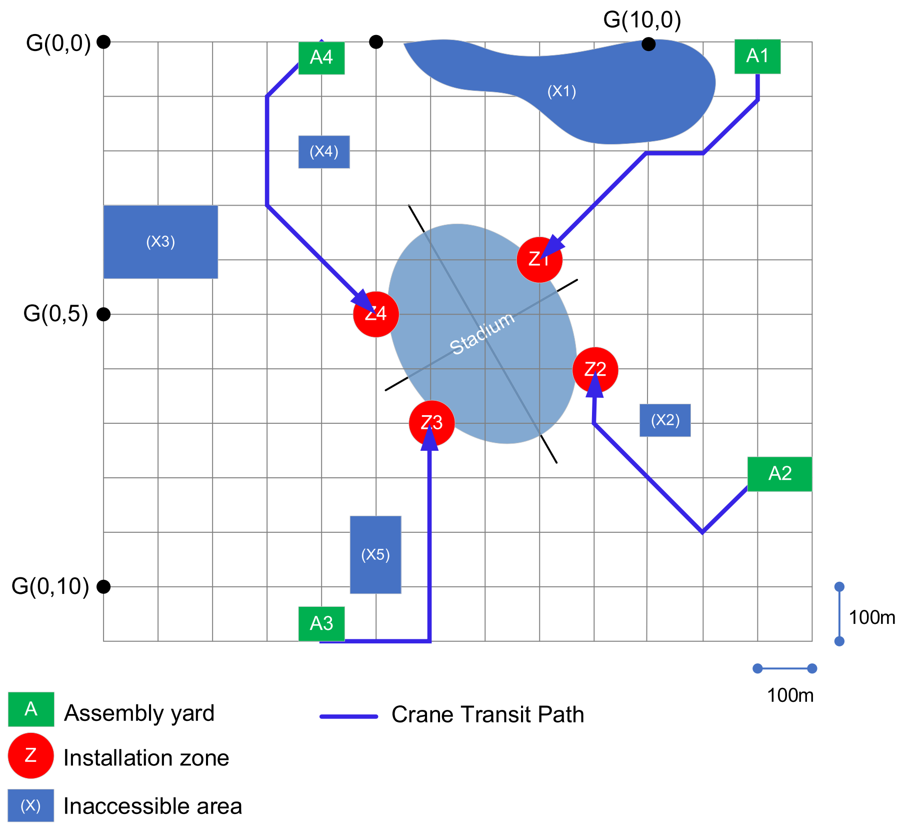

Fig. 7. Crane mat layout plan (transit path) prepared by proposed algorithm.

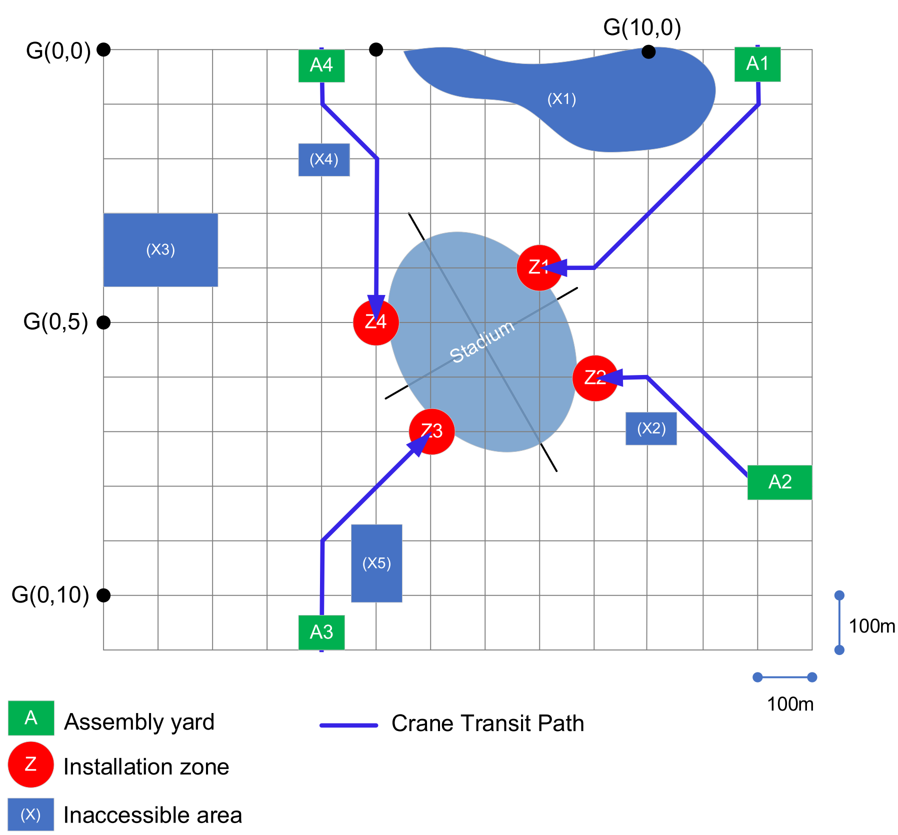

Fig. 8. Crane mat layout plan (transit path) prepared by shortest path algorithm.

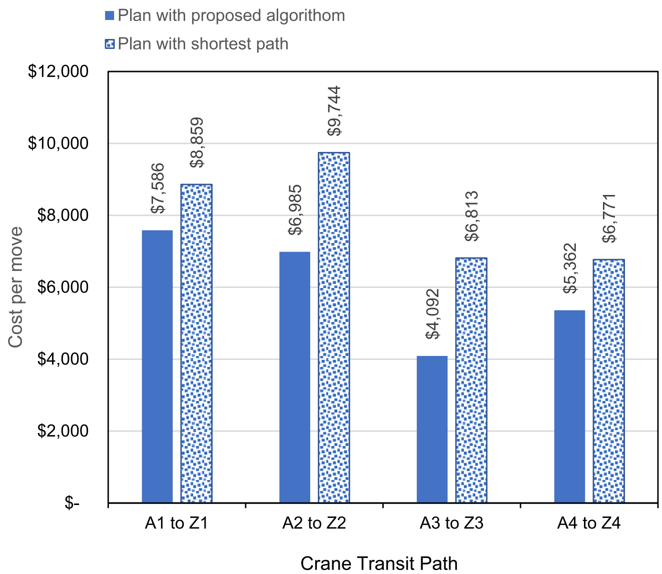

Fig. 9. Cost comparison between mat layout plan (crane transit path) generated by proposed methods and shortest possible path algorithm.

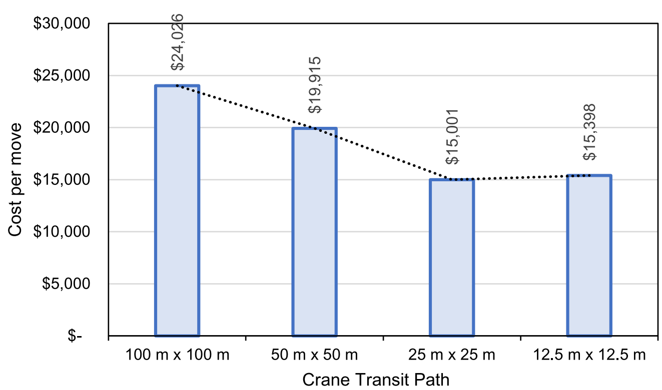

Fig. 10. Cost comparison of prosed plan with different grid sizes.

Table 8
the number of mats required for the planned job with 25 m × 25 m grid size.

Mat Size [length (m), thickness (mm)]	Travel length (m)	Mat Number (2.5 m width)
(3.5,45)	326.8	138
(3.75,50)	110.4	47
(4,55)	1115.7	469
(4.25,55)	1145.0	481
(4.5,60)	401.8	169
(5.5,70)	857.1	360
(6.75,85)	266.4	112
(7.75,90)	231.1	98

Appendix A. Appendix

Table A1
Path plan analysis results with different grid sizes with shortest path.

Grid size	Start coordinates	End coordinates (Destination)	Path	Planned Path	Cost per move ($/move)
50 m × 50 m	(0,24), (16,24), (22,8), (0,8)	(8,16), (12,18), (14,12), (10,10)	Path 1 (A1 – Z1)	(0, 24), (1, 24), (2, 24), (3,23), (4, 22), (4, 21), (4, 20), (5, 19), (6, 18), (7, 17), (8, 16)	6780
			Path 2 (A2 – Z2)	(16, 24), (16, 23), (16, 22), (16, 21), (15, 20), (14, 20), (13, 19), (12, 18)	5977
			Path 3 (A3 – Z3)	(22, 8), (21, 8), (20, 8), (19, 8), (18, 8), (17, 9), (16, 10), (15, 11), (14, 12)	3438
			Path 4 (A4 – Z4)	(0, 8), (1, 8), (2, 9), (3,10), (4, 10), (5, 10), (6, 10), (7, 10), (8, 10), (9, 10), (10,10)	6303
25 m × 25 m	(0,48), (32,48), (44,16), (0,16)	(16,32), (24,36), (28,24), (20,20)	Path 1 (A1 – Z1)	(0, 48), (1, 48), (2, 48), (3, 47), (4, 47), (5, 46), (6, 45), (7, 44), (8, 43), (9, 42), (10, 41), (11, 40), (12, 39), (13, 38), (14, 37), (15, 36), (15, 35), (15, 34), (15, 33), (16, 32)	6346
			Path 2 (A2 – Z2)	(32, 48), (32, 47), (32, 46), (32, 45), (32, 44), (32, 43), (31, 42), (30, 41), (29, 41), (28, 40), (27, 39), (26, 38), (25, 37), (24, 36)	4790
			Path 3 (A3 – Z3)	(44, 16), (43, 16), (42, 16), (41, 16), (40, 16), (39, 16), (38, 16), (37, 16), (36, 17), (35, 17), (34, 18), (33, 19), (32,20), (31,21), (30,22), (29, 23), (28, 24)	3162
			Path 4 (A4 – Z4)	(0, 16), (1, 16), (2, 16), (3, 17), (4, 17), (5, 18), (6, 19), (7, 19), (8, 19), (9, 19), (10, 19), (11, 19), (12, 19), (13, 19), (14, 19), (15, 19), (16, 19), (17, 19), (18, 19), (19, 19), (20,20)	3863
12.5 m × 12.5	(0,96), (76,96), (88,32), (0,32)	(32,64), (48,72), (56,48), (40,40)	Path 1 (A1 – Z1)	(0, 96), (1, 96), (2, 96), (3, 96), (4, 96), (5, 96), (6, 96), (7, 96), (8, 95), (9, 94), (10, 93), (11, 92), (12, 91), (13, 90), (14, 89), (14, 88), (15, 87), (15, 86), (16, 85), (17, 84), (18, 83), (19, 82), (20, 81), (21, 80), (22, 79), (23, 78), (24, 77), (25, 76), (26, 75), (27, 74), (28, 73), (29, 72), (29, 71), (29, 70), (29, 69), (29, 68), (29, 67), (30, 66), (31, 65), (32, 64)	6297
			Path 2 (A2 – Z2)	(76, 96), (75, 96), (74, 95), (73, 94), (72, 93), (71, 92), (70, 91), (69, 90), (68, 89), (67, 88), (66, 87), (65, 86), (64, 85), (63, 84), (62, 83), (61, 83), (60, 83), (59, 83), (58, 82), (57, 81), (56, 80), (55, 79), (54, 78), (53, 77), (52, 76), (51, 75), (50, 74), (49, 73), (48, 72)	3080
			Path 3 (A3 – Z3)	(88, 32), (87, 32), (86, 32), (85, 32), (84, 32), (83, 32), (82, 32), (81, 32), (80, 32), (79, 32), (78, 32), (77, 32), (76, 32), (75, 32), (74, 32), (73, 33), (72, 34), (71, 35), (70, 36), (69, 36), (68, 36), (67, 37), (66, 38), (65, 39), (64, 40), (63, 41), (62, 42), (61, 43), (60, 44), (59, 45), (58, 46), (57, 47), (56, 48)	5360
			Path 4 (A4 – Z4)	(0,32), (1,32), (2,32), (3,32), (4, 32), (5, 32), (6, 33), (7, 34), (8, 35), (9, 36), (10, 37), (11, 38), (12, 38), (13, 38), (14, 38), (15, 38), (16, 38), (17, 39), (18, 39), (19, 39), (20, 39), (21, 39), (22, 39), (23, 39), (24, 39), (25, 39), (26, 39), (27, 39), (28, 39), (29, 39), (30, 39), (31, 39), (32, 39), (33, 39), (34, 39), (35, 39), (36, 39), (37, 39), (38, 39), (39, 39), (40, 40)	3708

Table A2
Path plan analysis results with different grid sizes with proposed planning algorithm.

Grid size	Start coordinates	End coordinates (Destination)	Path	Planned Path	Cost per move ($/move)
50 m × 50 m	(0,24), (16,24), (22,8), (0,8)	(8,16), (12,18), (14,12), (10,10)	Path 1 (A1 – Z1)	(0, 24), (1, 24), (2, 24), (3, 23), (4, 22), (4, 21), (5, 20), (6, 19), (6, 18), (7, 17), (8, 16)	6780
			Path 2 (A2 – Z2)	(16, 24), (17, 23), (17, 22), (16, 21), (15, 20), (14, 19), (13, 18), (12, 18)	4632
			Path 3 (A3 – Z3)	(22, 8), (22, 9), (22,10), (21,11), (20,12), (19, 12), (18, 12), (17, 12), (16, 12), (15, 12), (14, 12)	3788
			Path 4 (A4 – Z4)	(0, 8), (1, 8), (2, 7), (3, 6), (4, 6), (5, 6), (6, 7), (7, 8), (8, 8), (9, 9), (10, 10)	4715
25 m × 25 m	(0,48), (32,48), (44,16), (0,16)	(16,32), (24,36), (28,24), (20,20)	Path 1 (A1 – Z1)	(0, 48), (1, 48), (2, 48), (3, 48), (4, 47), (5, 46), (6, 45), (7, 44), (7, 43), (7, 42), (7, 41), (7, 40), (7, 39), (7, 38), (8, 37), (9, 36), (10, 35), (11, 35), (12, 35), (13, 34), (14, 33), (15, 32), (16, 32)	5789
			Path 2 (A2 – Z2)	(32, 48), (33, 47), (33, 46), (33, 45), (33, 44), (32, 43), (31, 42), (30, 41), (29, 40), (28, 39), (27, 38), (26, 37), (25, 36), (24, 36)	3455
			Path 3 (A3 – Z3)	(44, 16), (43, 17), (42, 18), (41, 19), (41, 20), (41, 21), (41, 22), (40, 23), (39, 23), (38, 23), (37, 23), (36, 23), (35, 23), (34, 23), (33, 24), (32, 24), (31, 24), (30, 24), (29, 24), (28, 24)	1894
			Path 4 (A4 – Z4)	(0, 16), (1, 16), (2, 16), (3, 16), (4, 17), (5, 18), (6, 19), (7, 19), (8, 19), (9, 19), (10, 19), (11, 19), (12, 19), (13, 19), (14, 19), (15, 19), (16, 19), (17, 19), (18, 19), (19, 19), (20, 20)	3863
12.5 m × 12.5	(0,96), (76,96), (88,32), (0,32)	(32,64), (48,72), (56,48), (40,40)	Path 1 (A1 – Z1)	Path 1: [(0, 96), (1, 96), (2, 96), (3, 96), (4, 95), (5, 94), (6, 93), (7, 92), (8, 92), (9, 92), (10, 92), (11, 92), (12, 91), (13, 90), (14, 89), (14, 88), (14, 87), (14, 86), (14, 85), (14, 84), (14, 83), (14, 82), (14, 81), (14, 80), (14, 79), (14, 78), (14, 77), (14, 76), (14, 75), (15, 74), (16, 73), (17, 72), (18, 71), (19, 71), (20, 71), (21, 71), (22, 71), (23, 71), (24, 71), (25, 70), (26, 69), (27, 68), (28, 67), (29, 66), (30, 65), (31, 64), (32, 64)]	5577

(continued on next page)

Table A2 (*continued*)

Grid size	Start coordinates	End coordinates (Destination)	Path	Planned Path	Cost per move ($/move)
			Path 2 (A2 – Z2)	Path 2: [(76, 96), (75, 95), (74, 94), (73, 93), (72, 92), (71, 91), (70, 90), (69, 89), (68, 88), (67, 87), (66, 86), (65, 85), (64, 85), (63, 85), (62, 84), (61, 83), (60, 83), (59, 82), (58, 81), (57, 80), (56, 79), (55, 78), (54, 77), (53, 76), (52, 75), (51, 74), (50, 73), (49, 72), (48, 72)]	3011
			Path 3 (A3 – Z3)	Path 3: [(88, 32), (88, 33), (88, 34), (87, 35), (87, 36), (87, 37), (87, 38), (87, 39), (87, 40), (86, 41), (85, 42), (84, 43), (83, 44), (82, 45), (81, 46), (80, 46), (79, 46), (78, 46), (77, 46), (76, 46), (75, 46), (74, 46), (73, 46), (72, 46), (71, 46), (70, 46), (69, 46), (68, 46), (67, 46), (66, 47), (65, 48), (64, 48), (63, 48), (62, 48), (61, 48), (60, 48), (59, 48), (58, 48), (57, 48), (56, 48)]	3073
			Path 4 (A4 – Z4)	Path 4: [(0, 32), (1, 32), (2, 32), (3, 32), (4, 32), (5, 33), (6, 33), (7, 34), (8, 35), (9, 36), (10, 37), (11, 38), (12, 38), (13, 38), (14, 38), (15, 38), (16, 38), (17, 38), (18, 38), (19, 38), (20, 38), (21, 38), (22, 38), (23, 38), (24, 38), (25, 38), (26, 38), (27, 38), (28, 38), (29, 38), (30, 38), (31, 39), (32, 39), (33, 40), (34, 41), (35, 41), (36, 41), (37, 41), (38, 41), (39, 41), (40, 40)]	3736

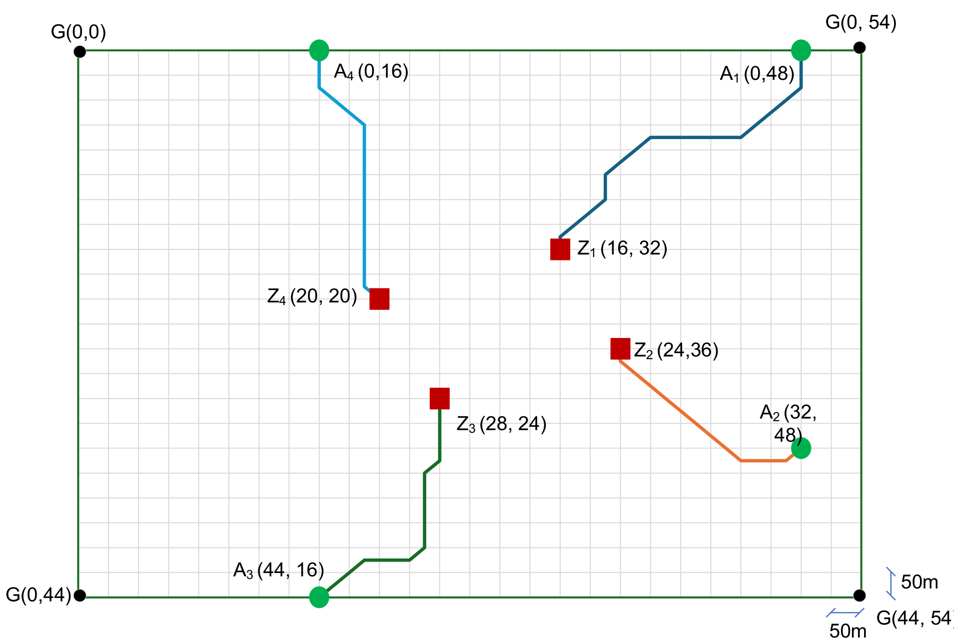

Fig. A1. The proposed crane path plan with 25 m × 25 m grid size.

Data availability

The model, or code that supports the findings of this study are also available from the corresponding author upon reasonable request. Data tables generated in this study can be found in this link: https://shorturl.at/PKyW3

References

[1] C. Rausch, M. Nahangi, M. Perreault, C.T. Haas, J. West, Optimum assembly planning for modular construction components, J. Comput. Civ. Eng. 31 (1) (2017) 04016039, https://doi.org/10.1061/(asce)cp.1943-5487.0000605.
[2] A.G. Gibb, Off-Site Fabrication: Prefabrication, Pre-Assembly and Modularisation, John Wiley & Sons, 1999. ISBN-13: 978–0470378366.
[3] A. Shapira, G. Lucko, C.J. Schexnayder, Cranes for building construction projects, J. Constr. Eng. Manag. 133 (9) (2007) 690–700, https://doi.org/10.1061/(asce)0733-9364(2007)133:9(690).
[4] X. Liu, D.H. Chan, B. Gerbrandt, Bearing capacity of soils for crawler cranes, Can. Geotech. J. 45 (9) (2008) 1282–1302, https://doi.org/10.1139/T08-056.
[5] G.M. Ali, A. Mansoor, S. Liu, J. Olearczyk, A. Bouferguene, M. Al-Hussein, Decision support for hydraulic crane stabilization using combined loading and crane mat strength analysis, Autom. Constr. 131 (2021) 103884, https://doi.org/10.1016/j.autcon.2021.103884.
[6] G.M. Ali, A. Bouferguene, M. Al-Hussein, Crane mat layout optimization based on agent-based greedy and reinforcement-learning approach, J. Constr. Eng. Manag. 149 (8) (2023) 04023067, https://doi.org/10.1061/jcemd4.coeng-12891.
[7] H. Taghaddos, U. Hermann, A.B. Abbasi, Automated crane planning and optimization for modular construction, Autom. Constr. 95 (2018) 219–232, https://doi.org/10.1016/j.autcon.2018.07.009.
[8] A. ElNimr, M. Fagiar, Y. Mohamed, Two-way integration of 3D visualization and discrete event simulation for modeling mobile crane movement under dynamically changing site layout, Autom. Constr. 68 (2016) 235–248, https://doi.org/10.1016/j.autcon.2016.05.013.
[9] N. Kayhani, H. Taghaddos, A. Mousaei, S. Behzadipour, U. Hermann, Heavy mobile crane lift path planning in congested modular industrial plants using a robotics approach, Autom. Constr. 122 (2021), https://doi.org/10.1016/j.autcon.2020.103508.
[10] A. Mousaei, H. Taghaddos, A. Nekouvaght Tak, S. Behzadipour, U. Hermann, Optimized mobile crane path planning in discretized polar space, J. Constr. Eng. Manag. 147 (5) (2021) 04021036, https://doi.org/10.1061/(ASCE)CO.1943-7862.0002033.
[11] W.H. Chan, M. Lu, J.P. Zhang, Attaining cost efficiency in constructing sports facilities for Beijing 2008 Olympic games by use of operations simulation, in: Proceedings - Winter Simulation Conference, 2006, pp. 2063–2070, https://doi.org/10.1109/WSC.2006.322994.
[12] D. Duerr, Effective bearing length of crane mats, in: Crane and Rigging Conference, Houston, Texas. Organized by Association of Crane and Rigging Professionals, Wixom, Michigan, USA, 2010, https://doi.org/10.13140/RG.2.2.21044.67200.

[13] Q. Zhao, Cause Analysis of US Crane-Related Accidents, Master of Science Thesis, Department of Building Construction, University of Florida, 2011, https://ufdc.ufl.edu/UFE0042972/00001/pdf.

[14] R.A. King, Analysis of Crane and Lifting Accidents in North America From 2004 to 2010, Master of Engineering Thesis, Department of Civil and Environmental Engineering. Massachusetts Institute of Technology, 2012, http://hdl.handle.net/1721.1/73792.

[15] J.E. Beavers, J.R. Moore, R. Rinehart, W.R. Schriver, Crane-related fatalities in the construction industry, J. Constr. Eng. Manag. 132 (9) (2006) 901–910, https://doi.org/10.1061/(asce)0733-9364(2006)132:9(901).

[16] BSL, Fatal occupational injuries involving cranes, in: Fact Sheet - Injuries, Illnesses, and Fatalities, U.S. Bureau of Labor Statistics, 2023. https://www.bls.gov/iif/factsheets/fatal-occupational-injuries-cranes-2011-17.htm. accessed on 21 December 2024.

[17] C. Chiang, B. Owen, Crane Accidents 'a Huge Concern' after Fourth Incident in Metro Vancouver, Canadian Underwriter, Newcom Media Inc, 2024. https://www.canadianunderwriter.ca/construction/crane-accidents-a-huge-concern-after-fourth-incident-in-metro-vancouver-1004243559/ (accessed on: 21 December 2024).

[18] M.F. Milazzo, G. Ancione, V.S. Brkic, D. Vališ, Investigation of crane operation safety by analysing main accident causes, in: *Risk, Reliability and Safety*, Innovating Theory and Practice, Walls, Revie & Bedford, Taylor & Francis Group, London, 2016, pp. 74–80. ISBN 978-1-138-02997-2, https://www.researchgate.net/profile/Maria-Francesca-Milazzo/publication/311439947_Investigation_of_crane_operation_safety_by_analysing_main_accident_causes/links/5867e59d08ae6eb871b751d8/Investigation-of-crane-operation-safety-by-analysing-main-accident-causes.pdf. Accessed from:.

[19] E. Gharaie, H. Lingard, T. Cooke, Causes of fatal accidents involving cranes in the Australian construction industry, Construct. Econ. Build. 15 (2) (2015) 1–12, https://doi.org/10.5130/AJCEB.v15i2.4244.

[20] A.R.A. Hamid, R. Azhari, R. Zakaria, E. Aminudin, R. Putra Jaya, L. Nagarajan, K. Yahya, Z. Haron, R. Yunus, Causes of crane accidents at construction sites in Malaysia, in: IOP Conference Series: Earth and Environmental Science vol. 220, No. 1, Institute of Physics Publishing, 2019, p. 012028, https://doi.org/10.1088/1755-1315/220/1/012028.

[21] G.Y.H. Yu, Forensic investigation on crane accidents, Int. J. Forens. Eng. 3 (4) (2017) 319, https://doi.org/10.1504/ijfe.2017.087671.

[22] D.E. Dickie, Crane Handbook, Construction Safety Association of Ontario, Ontario, Canada, 1990. ISBN 0–408–00455-2.

[23] S.S. Sulaiman, P. Leela Jancy, A. Muthiah, V. Janakiraman, S.J.P. Gnanaraj, An evolutionary optimal green layout design for a production facility by simulated annealing algorithm, in: Materials Today: Proceedings vol. 47, Elsevier Ltd, 2021, pp. 4423–4430, https://doi.org/10.1016/j.matpr.2021.05.256.

[24] Z. Zhang, W. Pan, Lift Planning and Optimization in Construction: A Thirty-Year Review. Automation in Construction, Elsevier B.V, 2020, https://doi.org/10.1016/j.autcon.2020.103271.

[25] M. Al-Hussein, S. Alkass, O. Moselhi, An algorithm for mobile crane selection and location on construction sites, Constr. Innov. 1 (2) (2001) 91–105, https://doi.org/10.1108/14714170110814532.

[26] H. Safouhi, M. Mouattamid, U. Hermann, A. Hendi, An algorithm for the calculation of feasible mobile crane position areas, Autom. Constr. 20 (4) (2011) 360–367, https://doi.org/10.1016/j.autcon.2010.11.006.

[27] H.R. Reddy, K. Varghese, Automated path planning for mobile crane lifts, Comput. Aided Civ. Inf. Eng. 17 (6) (2002) 439–448, https://doi.org/10.1111/0885-9507.00005.

[28] M.S.A.D. Ali, N.R. Babu, K. Varghese, Collision free path planning of cooperative crane manipulators using genetic algorithm, J. Comput. Civ. Eng. 19 (2) (2005) 182–193, https://doi.org/10.1061/(asce)0887-3801(2005)19:2(182).

[29] Y. Lin, D. Wu, X. Wang, X. Wang, S. Gao, Lift path planning for a nonholonomic crawler crane, Autom. Constr. 44 (2014) 12–24, https://doi.org/10.1016/j.autcon.2014.03.007.

[30] Bo Peng, Forest Lee Flager, Jiaao Wu, A method to optimize mobile crane and crew interactions to minimize construction cost and time, Automation in Construction 95 (2018) 10–19, https://doi.org/10.1016/j.autcon.2018.07.015.

[31] S. Hasan, M. Al-Hussein, U.H. Hermann, H. Safouhi, Interactive and dynamic integrated module for mobile cranes supporting system design, J. Constr. Eng. Manag. 136 (2) (2010) 179–186, https://doi.org/10.1061/(asce)co.1943-7862.0000121.

[32] C. Sydora, Z. Lei, M.F.F. Siu, S.H. Han, U. Hermann, Critical lifting simulation of heavy industrial construction in gaming environment, Facilities 39 (1–2) (2021) 113–131, https://doi.org/10.1108/F-08-2019-0088.

[33] K. Aghajamali, A. Nekouvaght Tak, H. Taghaddos, A. Mousaei, S. Behzadipour, U. Hermann, Planning of Mobile crane walking operations in congested industrial construction sites, J. Constr. Eng. Manag. 149 (7) (2023), https://doi.org/10.1061/jcemd4.coeng-13109.

[34] P. Cai, Y. Cai, I. Chandrasekaran, J. Zheng, Parallel genetic algorithm based automatic path planning for crane lifting in complex environments, Autom. Constr. (2016), https://doi.org/10.1016/j.autcon.2015.09.007.

[35] A. Mousaei, H. Taghaddos, S. Marzieh Bagheri, U. Hermann, Optimizing heavy lift plans for industrial construction sites using Dijkstra's algorithm, J. Constr. Eng. Manag. 147 (11) (2021), https://doi.org/10.1061/(asce)co.1943-7862.0002157.

[36] S. Even, Graph Algorithms, 2nd ed., Cambridge University Press, New York, USA, 2011 (ISBN 0521736536.).

[37] N. Deo, Graph Theory with Applications to Engineering and Computer Science, Courier Dover Publications; Prentice-Hall, Inc., Englewood Cliffs, New Jersey, 2016. ISBN 9780486807935.

[38] E.W. Dijkstra, A note on two problems in connexion with graphs, Numer. Math. 1 (1) (1959) 269–271, https://doi.org/10.1007/BF01386390.

[39] T.H. Cormen, C.E. Leiserson, R.L. Rivest, C. Stein, Introduction to Algorithms, 3rd ed., MIT Press, Cambridge, Massachusetts, USA, 2009. ISBN: 9780262533058.

[40] A. Pradhan, G. Mahinthakumar, (Kumar)., Finding all-pairs shortest path for a large-scale transportation network using parallel Floyd-Warshall and parallel Dijkstra algorithms, J. Comput. Civ. Eng. 27 (3) (2013) 263–273, https://doi.org/10.1061/(asce)cp.1943-5487.0000220.

[41] Sivakumar, PL., Varghese, K., & Babu, N. R. (2003). Automated path planning of cooperative crane lifts using heuristic search. J. Comput. Civ. Eng., 17(3), 197–207. doi:https://doi.org/10.1061/(asce)0887-3801(2003)17:3(197).

[42] J.M. Torres, L. Duenas-Osorio, Q. Li, A. Yazdani, Exploring topological effects on water distribution system performance using graph theory and statistical models, J. Water Resour. Plan. Manag. 143 (1) (2017), https://doi.org/10.1061/(asce)wr.1943-5452.0000709.

[43] C. Liu, M. Lu, Optimizing earthmoving job planning based on evaluation of temporary haul road networks design for mass earthworks projects, J. Constr. Eng. Manag. 141 (3) (2015), https://doi.org/10.1061/(asce)co.1943-7862.0000940.

[44] R. El Meouche, M. Abunemeh, I. Hijaze, A. Mebarki, I. Shahrour, Developing optimal paths for evacuating risky construction sites, J. Constr. Eng. Manag. 144 (2) (2018), https://doi.org/10.1061/(asce)co.1943-7862.0001413.

[45] J. Vaughan, W. Singhose, D. Kim, Analysis of unrestrained crawler-crane counterweights during tip-over accidents, Mech. Based Des. Struct. Mach. 50 (6) (2022) 2006–2031, https://doi.org/10.1080/15397734.2020.1768113.

[46] OCCUPATIONAL HEALTH AND SAFETY CODE, Alberta Regulation 191/2021, Office Consolidation © 2024, Government of Alberta, Retrived from: https://kings-printer.alberta.ca/documents/OHS/OHSCode_December_2024.pdf.

[47] CSA Z150:20 (2020). National Standard of Canada Safety code on mobile cranes, Canadian Standards Association, Toronto, Ontario, Canada, ISBN 978-1-4883-2913-5.

[48] X. Wang, Y.S. Lin, D. Wu, C.W. Zhang, X.K. Wang, Path planning for crane lifting based on bi-directional RRT, Adv. Mater. Res. 446–449 (2012) 3820–3823, https://doi.org/10.4028/scientific5/amr.446-449.3820.

[49] IHSA, Hoisting and Rigging Safety Manual, Infrastructure Health & Safety Association, Etobicoke, Ontario, Canada, 2020. ISBN-13: 978-0-919465-70-1.

[50] E. Barnett, C. Gosselin, A Bisection Algorithm for Time-Optimal Trajectory Planning along Fully Specified Paths, IEEE Transactions on Robotics 37 (1) (2021) 131–145, https://doi.org/10.1109/TRO.2020.3010632.

[51] E. Väljaots, H. Lehiste, M. Kiik, T. Leemet, Soil sampling automation using mobile robotic platform, Agron. Res. 16 (3) (2018) 917–922, https://doi.org/10.15159/AR.18.138.

[52] I. Catapano, G. Gennarelli, G. Ludeno, C. Noviello, G. Esposito, F. Soldovieri, Contactless ground penetrating radar imaging: state of the art, challenges, and microwave tomography-based data processing, IEEE Geosci. Remote Sens. Mag. 10 (1) (2022) 251–273, https://doi.org/10.1109/MGRS.2021.3082170.

[53] W. Wai-Lok Lai, X. Dérobert, P. Annan, A review of ground penetrating radar application in civil engineering: a 30-year journey from locating and testing to imaging and diagnosis, NDT&E Int. 96 (2018) 58–78, https://doi.org/10.1016/j.ndteint.2017.04.002.